JOURNAL OF PHYSICAL ORGANIC CHEMISTRY
J. Phys. Org. Chem. 2003; **16:** 891–899
Published online in Wiley InterScience (www.interscience.wiley.com). DOI: 10.1002/poc.680

New permanently charged phenanthridinium–nucleobase conjugates. Interactions with nucleotides and polynucleotides and recognition of ds-polyAH$^+$

Lidija-Marija Tumir,[1] Ivo Piantanida,[1] Iva Juranović Cindrić,[2] Tomica Hrenar,[2] Zlatko Meić[2] and Mladen Žinić[1]*

[1] Laboratory of Supramolecular and Nucleoside Chemistry, Division of Organic Chemistry and Biochemistry, Ruđer Bošković Institute, P.O.B. 180, HR 10002 Zagreb, Croatia
[2] Laboratory of Analytical Chemistry, Department of Chemistry, Faculty of Science, Strossmayerov trg14, HR 10000 Zagreb, Croatia

Received 3 March 2003; revised 4 June 2003; accepted 13 June 2003

ABSTRACT: *N*-Methyl-8-aminophenathridinium–uracil and –adenine conjugates possessing a nucleobase attached at the phenanthridinium 8-amino group by a trimethylene spacer were prepared in the form of water-soluble hydrogensulfate salts. Spectroscopic characteristics of the conjugates reveal the formation of folded conformations in water characterized by intramolecular aromatic stacking between the phenanthridinium unit and the tethered nucleobase. The conjugates form 1:1 complexes in water with either complementary or non-complementary nucleotides, giving log K_s values between 1 and 2 and showing a lack of any base recognition. Also, the binding studies with single-stranded polynucleotides showed no preference of conjugates to polynucleotides containing complementary nucleobases. At pH 5, the *N*-methylphenanthridinium–adenine conjugate exhibited preferred binding to double-stranded (ds-) polyAH$^+$, whereas its protonated analogue bound preferably to polyU. The results reveal that the presence of protonated or permanently charged intercalator units in the conjugates dramatically changes their binding preferences for polynucleotides. Copyright © 2003 John Wiley & Sons, Ltd.
Additional material for this paper is available from the epoc website at http://www.wiley.com/epoc

KEYWORDS: phenanthridinium–adenine conjugate; ds-polyAH$^+$; nucleotides; polynucleotides

INTRODUCTION

Intensive research during the last two decades has shown that single-stranded (ss-) domains of DNA and RNA are of the paramount importance for life processes in living cells.[1,2] Among different types of ss-domains, the abasic sites have attracted a lot of interest owing to their important role in the DNA repair system.[3] Since many of the antitumor drugs act by modifying (i.e. alkylating) nucleobases in DNA,[4] molecules that bind specifically at such lesions and inhibit the DNA repair system may potentiate the action of antitumor drugs.[5] The importance of adenine in the study of abasic sites can be demonstrated by *in vitro* experiments with DNA polymerases. Namely, polymerases preferentially incorporate dA opposite to an abasic site (the so-called 'A-rule'), a selectivity that is not fully understood and cannot be explained by thermodynamic or structural studies.[6] In the last decade, pH-dependent properties of nucleobases, especially adenine and cytosine, have also been a subject of intensive research.[7] It has been shown that the pK_a value of adenine at the N1 position (see Fig. 1) is strongly dependent on the local surroundings such as stacking interactions, possibility of participation in hydrogen bonding and charge stabilization. Protonated adenine readily forms a number of different types of hydrogen bonds, resulting in a variety of non-canonical base pairs of high biological importance.[7] In a number of recent publications, the synthesis of molecules designed for recognition of DNA abasic sites has been reported.[8] The molecules incorporate three structural units: (a) an intercalator unit for strong binding to DNA, (b) a nucleic base for recognition of the complementary non-paired base at the abasic site and (c) a linker connecting the intercalator and the base of a suitable length and flexibility to allow pairing of a tethered base with that at the abasic site. In addition to binding at abasic sites, one paper also describes the recognition of *n*-propyladenine by proflavine–thymine conjugate in aqueous media. However, it was pointed out that there was no direct evidence of hydrogen bonding between complementary

**Correspondence to:* M. Žinić, Laboratory of Supramolecular and Nucleoside Chemistry, Division of Organic Chemistry and Biochemistry, Ruđer Bošković Institute, P.O.B. 180, HR 10002 Zagreb, Croatia. E-mail: zinic@irb.hr

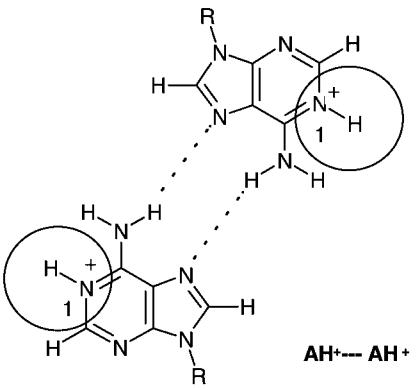

Figure 1. Hydrogen bonding between protonated adenines (N1) in ds-polyAH$^+$

nucleobases.[9] It appears that this type of conjugate may also act as receptor molecules capable of recognizing complementary nucleosides or nucleotides in water or may bind strongly to ss-polynucleotides at sequences containing complementary bases. Intrigued by the possibility of nucleotide recognition by such conjugates, we have prepared a series of *N5*-protonated phenanthridinium–adenine and –uracil derivatives [Fig. 2(B)] with different lengths of aliphatic linkers and studied their interaction with nucleotides and polynucleotides in aqueous media.[10,11] Such conjugates showed a lack of any recognition of complementary nucleotides, but the adenine conjugate exhibited interesting selectivity toward complementary polyU.[11] Binding studies were performed at a non-physiological pH of 5, since the protonation of phenanthridine nitrogen was necessary to provide a sufficient solubility of the conjugates in water. In the next step, we synthesized the *N5*-methylated phenanthridinium conjugates shown in Fig. 2(A). Owing to the permanently charged phenanthridinium unit, such conjugates should be sufficiently soluble in water at the physiological pH of 7 and their binding preferences toward nucleotides and polynucleotides could be altered compared with those of the protonated phenanthridinium conjugates in acidic conditions. Here, we report on binding studies of uracil and adenine conjugates **7** and **8**, respectively, and on the reference derivative **6** lacking a tethered base with nucleotides and double-stranded (ds-) and ss-polynucleotides at pH 5 and 7. They all show that their binding preferences change dramatically with respect to those of the protonated analogues. We also report on the unique selective binding of **8** to the polyAH$^+$ double helix formed by polyA at pH 5. To find an explanation for the observed selectivity, a model of ds(AH$^+$)$_4$ with intercalated compound **8** was built and geometry optimizations were carried out using quantum chemical methods.

RESULTS AND DISCUSSION

Synthesis

As outlined in Scheme 1, trifluoromethylsulfonate salts **1** and **2** were prepared from the corresponding 8-tosyl-protected phenanthridines,[10] by reaction with an excess of methyl trifluoromethylsulfonate in dichloroethane (at room temperature, under argon) and subsequent deprotection by trifluoromethylsulphonic acid *in situ*.[12]

Compound **5**, however, could not be prepared in this way owing to the simultaneous methylation at one of

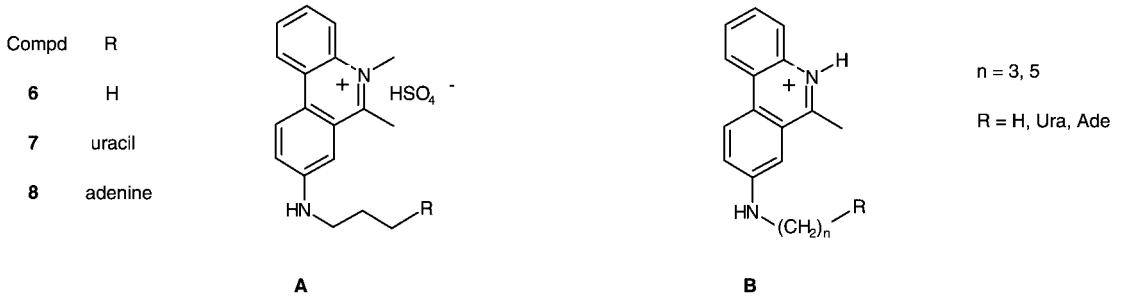

Figure 2. (A) Phenanthridinium–nucleobase conjugates **7** and **8** and the reference phenanthridinium derivative **6**; (B) previously studied *N5*-protonated phenathridinium analogues

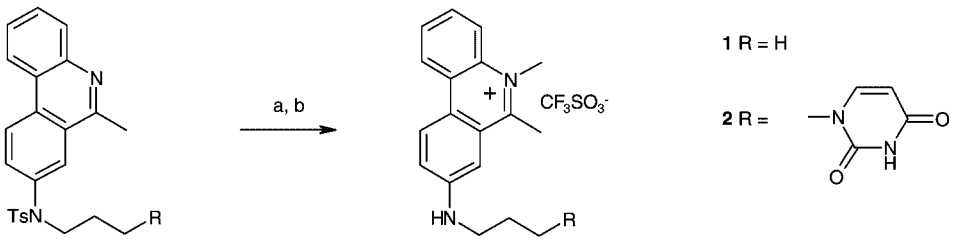

Scheme 1. (a) $CF_3SO_3CH_3$, $ClCH_2CH_2Cl$, Ar, r.t.; (b) CF_3SO_3H, $ClCH_2CH_2Cl$, Ar, r.t.

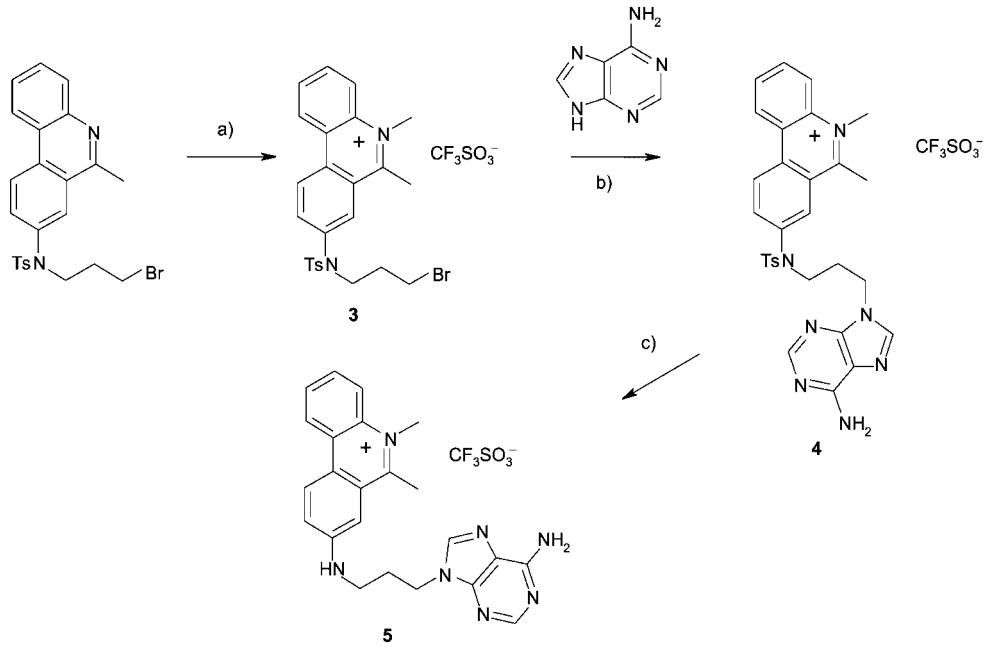

Scheme 2. (a) $CF_3SO_3CH_3$, $ClCH_2CH_2Cl$, Ar, r.t.; (b) NaH, dry DMF, Ar, r.t.; (c) CF_3SO_3H, $ClCH_2CH_2Cl$, Ar, r.t.

heterocyclic adenine nitrogens. Therefore, N5 of *N*-3-bromopropyl-*N*-tosyl-8-amino-6-methylphenanthridine was methylated in the first step, giving the triflate salt **3** in a 52% yield. In the next step, **3** was reacted with a large excess of adenine in the presence of NaH, giving the phenanthridinium salt **4** in 18% yield. Finally, the tosyl protection was removed by reaction with trifluoromethylsulfonic acid, to give **5** in a 80% yield (Scheme 2).

Exchange of lipophilic trifluoromethylsulphonate anion for hydrophilic hydrogensulfate was performed by mixing the acetonitrile solutions of compound **1**, **2** or **5** with a 10-fold excess of tetrabutylammonium hydrogensulfate in acetonitrile, yielding precipitation of the corresponding hydrogensulphate salts **6–8** [Fig. 2(A)].[13]

Spectroscopic properties

In the electronic absorption spectra of **6–8** taken from an aqueous solution, changes in absorbance obey the Lambert–Beer law in the concentration range 1×10^{-6}–1×10^{-4} mol dm^{-3}. The absorption maximum of **8** at 268 nm is blue shifted compared with reference **6** (Table 1), owing to the additive absorption maximum of the attached adenine ($\lambda_{max} = 262$ nm). The red shift of another absorption maximum of **8** ($\lambda_{max} = 449$ nm, Table 1) and a pronounced hypochromic effect compared with reference **6** strongly support intramolecular stacking interactions between the phenanthridinium unit and the tethered nucleobase. Hypochromicity observed in the spectra of uracil conjugate **7** vs reference **6** is less pronounced than that of **8** and there is almost no shift of maxima. The latter can be explained by the smaller aromatic surface of uracil compared with adenine and therefore weaker stacking interactions of the former with phenanthridinium moiety. It is interesting that the hypochromicity observed for permanently charged uracil conjugate **7** is significantly stronger than that found for the previously reported protonated phenanthridine–uracil analogue under the same experimental conditions.[10] Since the pK_a of all of the *N5*-protonated phananthridine

Table 1. Molar extinction coefficients, absorption maxima of **7**, **8** and references **6**, **Ade-C3** and **Ura-C3**, fluorescence emission intensities and maxima of **6–8** pH 7, Na cacodylate buffer, 0.04 mol dm^{-3}

	UV–Vis				Fluorescence emission		
Compound	λ_{max} (nm)	$\Delta\lambda_{max}$[a] (nm)	ε (mol^{-1} cm^2)	H (%)[b]	λ_{max} (nm)	$\Delta\lambda$[c] (nm)	Int(6)/Int(X)
6	279/438	—	44.16/4.26	—	575	—	—
7	278/438	−1/0	33.2/3.1	25/27	552	23	0.94
8	268/449	−11/+11	18.68/1.5	61/65	541	34	4.0
Ade-C3	262	—	13.73	—			
Ura-C3	267	—	9.92	—			

[a] Shift of the maxima calculated as λ_{max}(**6**) − λ_{max}(**7** or **8**).
[b] Hypochromic effect at $\lambda = 279$ nm estimated as: $\{[\varepsilon(\mathbf{6}) - \varepsilon(\mathbf{7} \text{ or } \mathbf{8})]/\varepsilon(\mathbf{6})\} \times 100$.
[c] $\Delta\lambda = \lambda(\mathbf{6}) - \lambda(\mathbf{7} \text{ or } \mathbf{8})$.

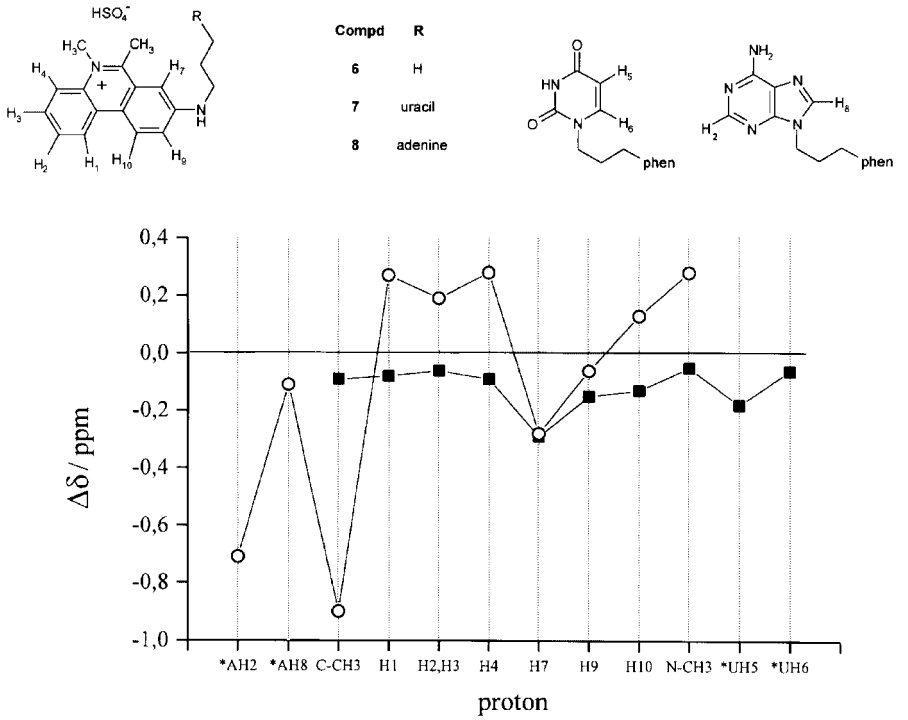

Figure 3. Induced chemical shifts $\Delta\delta$ (ppm) ($\Delta\delta_{phen} = \delta_{\mathbf{7,8}} - \delta_{\mathbf{6}}$, $^{*}\Delta\delta = \delta_{adenine\text{–}\mathbf{8},\ uracil\text{–}\mathbf{7}} - \delta_{Ade\text{-}C3,\ Ura\text{-}C3}$) by intramolecular self-stacking in **7** (■) and **8** (○)

conjugates is 6, close to 91% of the uracil conjugate should be protonated at pH 5.[10] Consequently, the observed difference in hypochromicity for **7** and its analogue, the protonated uracil conjugate, indicates that the strength of intramolecular stacking depends on the charge distribution of phenanthridinium units.

The fluorescence emission of **6–8** is linearly dependent on concentration up to 5×10^{-6} mol dm^{-3}. The excitation spectra of all compounds studied are in good agreement with their UV–visible spectra. The emission maxima of nucleobase conjugates **7** and **8** are significantly blue shifted compared with reference **6** (Table 1). Since the blue shift of ethidium bromide emission occurs upon its intercalation in ds-polynucleotides, the same observation for **7** and **8** additionally supports the intramolecular base-on-phenathridinium stacking. Again, the tethered adenine of **8** induced a significantly stronger emission change of the phenanthridinium unit than uracil of **7** (Table 1).

^{1}H NMR spectra of **6–8** in D_2O ($\sim 10^{-3}$ mol dm^{-3}) were fully assigned by means of one- and two-dimensional techniques and also by analogy with previously reported derivatives.[10] Taking into account the previously reported self-association constants K_{sa} for ethidium bromide (**EB**, $K_{sa} = 180$ mol^{-1} dm^{3})[14] and protonated phenanthridinium–nucleobase conjugates (estimated $K_{sa} = 10^{2}$ mol^{-1} dm^{3}),[10] only about 20% of self-association for **6–8** could be expected in the concentration range used for ^{1}H NMR measurements. However, the low solubility of the compounds and appearance of broad signals prevented the accumulation of sufficiently accurate NMR data for calculation of the self-association constants. Comparison of the chemical shifts of phenanthridinium protons of **7** and **8** with those of the reference derivative **6** reveals strong upfield shifts of the H7 and H9 protons of both nucleobase conjugates (Fig. 3).

The same observation has been reported for protonated phenanthridinium conjugates and was found to originate mostly from the intramolecular base-on-phenathridinium stacking interactions rather than from intermolecular stacking.[10] The tethered base protons of **7** and **8** also show significant upfield shifts relative to those of the reference derivatives Ade-C3 and Ura-C3 (Fig. 3). These findings are in accord with the results of UV–visible and fluorescence experiments, corroborating that both **7** and **8** form folded conformations with intramolecular base-on-phenathridinium stacking. The strongest upfield shift was observed for the phenanthridinium C6-methyl protons of **8**, indicating their close proximity to stacked adenine. The magnitude of shielding effects is higher for adenine conjugate **8** than for uracil conjugate **7**, which is in accord with previous observations of a stronger stacking of intercalators with purine than with pyrimidine nucleobases.[15,16]

Interactions with nucleotides

Addition of nucleotides to aqueous solutions of **6–8** induces significant changes in their fluorescence emission, allowing the determination of the binding constants ($\log K_s$, Table 2) and stoichiometries of the

Table 2. Binding constants ($\log K_s$) for **6–8** toward nucleotides[a,b]

Compound	AMP	ATP	GMP	UMP
6	1.6 ± 0.04	2.0 ± 0.1	2.00 ± 0.13	1.6[c]
7	1.7 ± 0.07	1.9 ± 0.04	2.1 ± 0.04	1.5[c]
8	2.1 ± 0.05	—	1.8 ± 0.06	1.7 ± 0.1
EB	1.6	—	1.6	1.2

[a] Fluorimetric titrations were performed at pH 6 ($I = 0.1\ \mathrm{mol\ dm^{-3}}$, Na cacodylate buffer).
[b] AMP^{2-} = adenosine monophosphate; ATP^{4-} = adenosine triphosphate; GMP^{2-} = guanosine monophosphate; UMP^{2-} = uridine monophosphate.
[c] Only 50% of complexation was reached, allowing only estimation of binding constant.

conjugate–nucleotide complexes. Processing the fluorescence titration data for **6–8** and various nucleotides gave the best fit for the 1:1 stoichiometry of complexes in each case. The calculated binding constants (K_s) were of the same order of magnitude as those found for ethidium bromide[15,16] and protonated phenanthridinium conjugates.[10] No significant charge dependence was observed for the binding of AMP^{2-}, ADP^{3-} and ATP^{4-} series either, suggesting the dominant role of intermolecular π–π stacking interactions between the phenanthridinium unit of the conjugate and a nucleobase of the nucleotide, and only a minor contribution of the electrostatic binding. No significantly different affinity of **7** and **8** toward complementary nucleotides was observed. Hence, as in the case of protonated phenanthridinium conjugates, no recognition of the complementary nucleotide could be achieved by permanently charged conjugates.

Interactions with polynucleotides

Spectroscopic titrations. Interactions of **6–8** with *ct* DNA as the representative of a ds-polynucleotide at pH 5 were studied by fluorimetric titrations. Addition of *ct* DNA resulted in a 3.4-fold increased emission of the reference compound **6** and only 1.7- and 1.6-fold that of **7** and **8**, respectively. For comparison, the fluorescence of **EB** (as reported previously)[17] increased 20-fold. The binding constants for **6–8** ($\log K_s = 5.2$–5.9) and [bound ligand]/[polynucleotide phosphate] ratios ($n = 0.08$–0.20) calculated from titration data according to the Scatchard equation[17,18] are similar to those determined for **EB** ($\log K_s = 6.1$, $n = 0.2$), within the error of the method.[19] These results show that the conjugates bind to *ct* DNA by intercalation with similar affinity as **EB** and that the presence of a spacer and a tethered nucleobase does not greatly alter the intercalation ability of phenanthridinium unit. Only slightly lower values of n determined for **8** relative to reference **6** and **EB** indicate a somewhat less dense intercalation, probably due to steric hindrance imposed by the linker and the adenine.

UV–visible and fluorimetric titrations of **6–8** with ss-polynucleotides were performed at physiological conditions (pH 7) and also at pH 5 for comparison with previously studied protonated analogues [Fig. 2(B)].[11] In all titrations, addition of ss-polynucleotide to the solutions of **6–8** induced a hypochromic effect in the UV–visible spectra and an increase in fluorescence (Table 3). In general, addition of polyA resulted in more pronounced spectroscopic changes than the addition of polyU. This observation can be explained by a larger aromatic surface and hence a stronger stacking between the phenanthridinium unit and purine nucleobases but it also points to stacking interactions being the dominant binding force that stabilizes such complexes.

Upon addition of polyA under acidic conditions (pH 5), the spectroscopic changes of **6–8** (hypochromic and bathochromic effects in UV–visible spectra and fluorescence increase) were significantly more pronounced than at a neutral pH. It is well known that protonated $polyAH^+$ at pH 5 forms a double helix (Fig. 1).[2b] In ds-helix, the base pairs provide a larger surface for stacking with intercalated phenanthridinium than single bases in ss-polyA at pH 7. In contrast, spectroscopic changes induced by addition of polyU were found to be independent of pH since the polynucleotide remained single-stranded at both pH values.

Table 3. Spectroscopic properties of complexes **6–8** with ss-polynucleotides[a]

		PolyA		PolyU	
Compound	pH	UV–Vis ΔA^b (%)	Fluorescence; ΔI^b [d] $\lambda_{exc} = 325/440$ nm (%)	UV–Vis ΔA^b (%)	Fluorescence; ΔI^b [d] $\lambda_{exc} = 325/440$ nm (%)
6		−35	+525/+170	−8	—[c]
7	5	−20	+310/+150	−15	—[c]
8		−10	+260/+120	−17	—[c]
6		−14	+200/+60	−12	—[c]
7	7	−20	+110/+40	−14	—[c]
8		−10	+90/+38	−3	—[c]

[a] Spectroscopic titrations were performed at pH 5 and 7 ($I = 0.1\ \mathrm{mol\ dm^{-3}}$, Na cacodylate buffer), λ_{max}(**6**, **7**) = 440 nm and λ_{max}(**8**) = 445 nm.
[b] Calculated as $\Delta A(\Delta I) = \{[A_0(I_0) - A(I)]/A_0(I_0)\} \times 100$, where $A(I)$ is calculated value at 100% of complex formed.
[c] Due to the linear dependence of spectroscopic changes on the concentration of polynucleotide, it was not possible to calculate $A(I)$ value at 100% of complex formed.
[d] Different excitation wavelengths (325 nm abs. shoulder; 440 nm abs. maxima) were used for the comparison of the observed emission changes.

Table 4. Binding constants ($\log K_s$) and ratios n ($c_{\text{bound } \mathbf{6–8}}/c_{\text{phosphate}}$)[a] for **6–8** towards ss-polynucleotides[b]

		PolyA		PolyU	
Compound	pH	n	$\log K_s$	n	$\log K_s$
6	5	0.1 ± 0.05	4.3 ± 0.1	—[c]	<3[c]
7		0.1 ± 0.05	4.8 ± 0.2	—[c]	<3[c]
8		0.1 ± 0.05	5.3 ± 0.2	—[c]	<3[c]
6	7	0.1 ± 0.05	4.8 ± 0.2	—[c]	<3[c]
7		0.1 ± 0.05	4.7 ± 0.2	—[c]	<3[c]
8		0.1 ± 0.05	4.4 ± 0.3	—[c]	<3[c]

[a] The correlation coefficients >0.999 correspond to given ranges of n and $\log K_s$.
[b] Fluorimetric titrations were performed at pH 5 and 7 ($I = 0.05$ mol dm^{-3}, Na cacodylate buffer).
[c] Estimated value owing to <20% of complex formed, $\lambda_{exc} = 320$ nm and $\lambda_{exc} = 440$ nm used for titration.

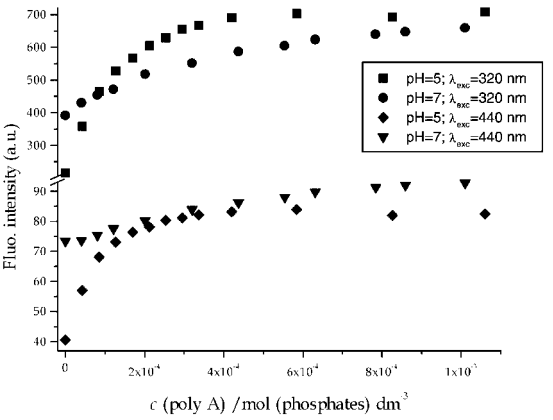

Figure 4. Fluorimetric titration of **8** with polyA at pH 5 and 7 ($I = 0.05$ mol dm^{-3}, Na cacodyate buffer) using two excitation wavelengths

The observed spectroscopic changes (bathochromic and hypochromic effects in UV–visible titrations and fluorescence increase) are more pronounced for the reference derivative **6** lacking a nucleobase and follow the order **8** < **7** < **6** (Table 3). The UV–visible and fluorimetric properties along with NMR results clearly suggest the formation of folded conformations of **7** and **8** in aqueous media. Owing to intramolecular base-on-phenanthridinium stacking, free **7** and **8** exhibit a lower absorbance, bathochromic shifs and lower emission intensities relative to **6** lacking a tethered base. Consequently, additional spectroscopic effects resulting from binding to polynucleotides should be less pronounced for **7** or **8** than for the reference **6**, showing in the free state a stronger absorbance, non-shifted phenanthridinium bands and higher emission intensity than the former conjugates.

No significantly increased affinity of conjugates **7** and **8** toward complementary ss-polynucleotide relative to the non-complementary one could be observed (Table 4). The binding constants for polyU complexes with **6–8** can only be estimated ($\log K_s < 3$, Table 4) owing to solubility problems at polyU concentrations >0.01 mol dm^{-3}. The affinity of **6** and the uracil conjugate **7** towards polyA is the same at pH 5 and 7. In contrast, the affinity of adenine conjugate **8** toward ds-polyAH$^+$ formed at pH 5 is an order of magnitude higher than that at pH 7 (Table 4, Fig. 4); the K_s of **8** is also significantly higher than those of **7** and the reference **6**. Interestingly, the affinity order reverses at pH 7. These results strongly suggest that some additional specific interactions stabilize the complex of **8** and ds-polyAH$^+$. To prove this additional stabilization, thermal denaturation experiments with **6**, **7** and **8** and polyA at pH 5 were performed.

The double helix of polyAH$^+$ formed at pH 5 under the applied experimental conditions exhibits a melting transition at 73 °C. Addition of adenine conjugate **8** resulted in strong stabilization of ds-polyAH$^+$ (Fig. 5: ΔT_m/ratio$_{\mathbf{8}/\text{polyAH}^+}$: 2.3/0.2; 4.6/0.3; 17.0/0.5), while addition of the reference compound **6** and the uracil conjugate **7** had no effect on the melting transition. Hence these results are clearly in accord with those of fluorimetric titrations for **8** and support the conclusion that the adenine conjugate **8** recognizes ds-polyAH$^+$ (Table 4).

To account for the observed enhanced binding of **8** to ds-polyAH$^+$, the molecular modelling was performed on the ds-polyAH$^+$–**8** intercalative complex.

The structure obtained is presented in Fig. 6. It shows that additional interaction, besides intermolecular stacking, is possible through hydrogen bonding between the adenine N1 hydrogen of ds-polyAH$^+$ and the adenine N-1 of **8**. These hydrogen bonds could explain the stronger binding of **8** and increased thermal stabilization of ds-polyAH$^+$.

Conjugate **8**, on binding to polyU, could form the pseudo-polyA–U complex by intercalation of phenanthridinium between adjacent uracils and formation of hydrogen bonds between adenine of **8** and the stacked uracil. To check this possibility, polyU saturated with adenine conjugate **8** (ratio$_{\text{polyU}/\mathbf{8}} \approx 1$) was prepared. However, no thermal melting transition was observed, showing that the

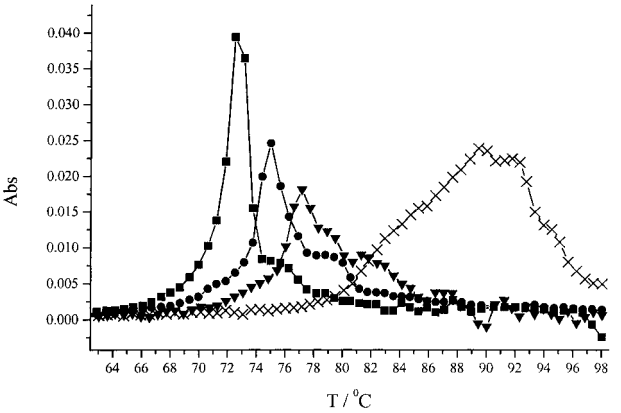

Figure 5. First derivative of melting curves of ds-polyAH$^+$ (■) and **8**–ds-polyAH$^+$ complexes at the **8**–ds-polyAH$^+$ ratios of 0.2 (●), 0.3 (▼) and 0.5 (x)

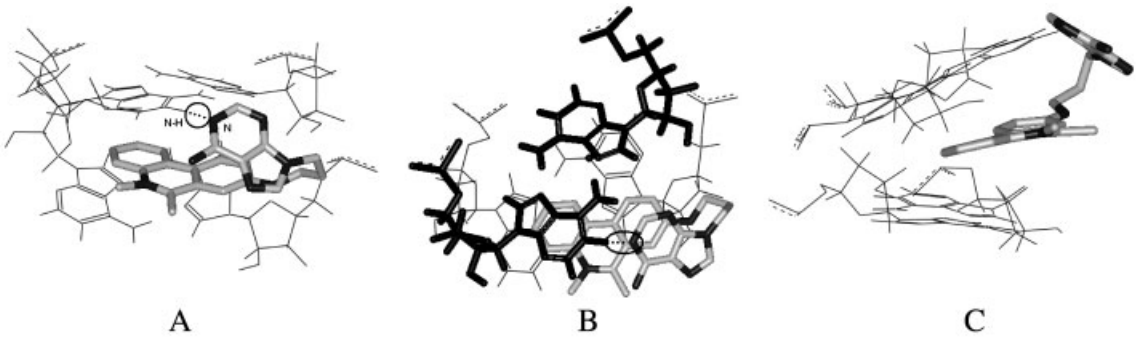

Figure 6. Optimized structure of ds-polyA$^+$ tetramer–**8** intercalative complex (only the middle two pairs of tetramers are shown; hydrogen atoms of **8** omitted for clarity). Possible hydrogen bonding between adjacent adenine $^+$N1-H and the N1 of **8** is indicated in (A) and (B) (distance 2.65 Å). In (C) the side view of the complex showing intercalation of the phenantridinium unit of **8** can be seen

pseudo-polyA–U complex was not formed. This result is also in agreement with the results of fluorimetric titrations, showing the absence of any increased affinity of **8** towards complementary polyU (Table 4).

CONCLUSION

The spectroscopic properties and conformational characteristics of novel phenanthridinium–nucleobase conjugates **6–8** are comparable to those of the previously studied protonated phenanthridine–nucleobase conjugates.[10] Folded conformations with intramolecularly base-on-phenanthridinium stacking were found for both series of conjugates. Intramolecular stacking is significantly more pronounced for the adenine conjugates than for the uracil conjugates, in accord with the known dependence of aromatic stacking on the surfaces in contact.[16]

There is no increased affinity of **7** and **8** towards complementary nucleotides, as already found for previously studied protonated phenanthridine–nucleobase conjugates.[10] These results are at variance with the reported recognition of propyladenine by proflavine–thymine conjugate in aqueous media.[9] Spectrophotometric titrations of **6–8** with ss- and ds-polynucleotides suggest intercalation as the dominant binding interaction of the phenanthridinium unit under both acidic (pH 5) and physiological (pH 7) conditions. The results of spectroscopic binding studies show a lack of any recognition of the complementary polynucleotides by conjugates **7** and **8** at both pH 5 and 7. Hence both the nucleotides and polynucleotides possessing bases complementary to those tethered to **7** and **8** could not be recognized by this type of intercalator–nucleobase conjugate. It can be concluded that the hydrogen bonding between complementary bases on the phenanthridinium surface is disfavored owing to strongly competitive hydration of H-bond donor and acceptor sites.

It was observed that, at pH 5, the adenine conjugate (**8**)–polyAH$^+$ complex is significantly more stable than the corresponding complexes of uracil conjugate **6** and the reference **7** lacking the nucleobase. This can be explained only by the additional interactions of the adenine of **8** with ds-polynucleotide. On the other hand, the results of binding studies for *N*-methylphenanthridinium derivative **8** and its protonated analogue B (Fig. 1, $n = 3$, R = Ade)[10] and polynucleotides reveal their different properties. The former exhibits a significantly stronger binding to ds-polyAH$^+$ and the latter to polyU. Although there is no definite explanation for the observed preferences at present, they could be a consequence of a different density and/or distribution of the positive charge on the phenanthridinium units of the protonated and methylated conjugates.

NMR spectra or x-ray structural analysis of the conjugate–short oligonucleotide complexes is necessary to provide a deeper insight into the specific interactions responsible for the observed selectivity of **8** toward ds-polyAH$^+$ and its protonated analogue toward polyU. Research along this line is in progress. However, relying upon experimental data presented in this and previously reported papers,[10,11] we can stress the importance of small structural and charge variations in the conjugates, which can result in a dramatic change of their binding preferences toward polynucleotides. Such variations, however, seem to be less important for binding of simple nucleotides in water. The results presented provide new experimental facts relating to the structure and charge of nucleic acid binders of intercalator–nucleobase conjugate type that can be of high relevance for design of small molecules capable of recognizing specific ss-regions of DNA and RNA.

EXPERIMENTAL

General procedures. ^{1}H NMR spectra were recorded on a Varian Gemini 300 spectrometer operating at 300 MHz. Chemical shifts (δ) are expressed in ppm and J values in Hz. Signal multiplicities are denoted as s (singlet), d (doublet), t (triplet), q (quartet) and m (multiplet).

Electron absorption spectra were recorded on a Varian Cary 3 spectrometer using quartz cuvettes (1 cm). Fluorescence spectra were recorded on a Perkin-Elmer LS 50 fluorimeter. Mass spectra were obtained using an Extrel 2001DD spectrometer. Preparative thin-layer chromatography (TLC) was carried out using Merck Kieselgel HF_{254} plates. Melting-points for phenanthridinium salts were not determined, since these salts melt in a broad temperature range (170–210 °C for triflate salts, 200–280 °C for hydrogensulfate salts) followed by darkening of the sample, that is caused by decomposition of the permethylated phenanthridinium salt. For all products, purity was checked by ^{1}H NMR spectroscopy. In several cases, a correct elemental analysis could not be obtained owing to the polar and hygroscopic character of compounds. Spectroscopic data (^{1}H NMR, ^{13}C NMR, HRMS, ESMS) are available as Supplementary Material at the epoc website at http://www.wiley.com/epoc.

UV–visible and fluorescence measurements. Nucleotides and polynucleotides were purchased from Sigma and Aldrich and used without further purification. Polynucleotides were dissolved in sodium cacodylate buffer, 0.05 mol dm^{-3}, pH 7, and their concentrations were determined spectroscopically as the concentration of phosphates. The measurements were performed in aqueous buffer solution (sodium cacodylate–HCl, 0.05 mol dm^{-3}, pH 5–7). Under the experimental conditions used, the absorbance and fluorescence intensities of **6–8** were proportional to their concentrations. Spectroscopic titrations were performed at constant ionic strength (sodium chloride, 0.1 mol dm^{-3}) by adding portions of nucleotide or polynucleotide solution to solutions of the tested compound. The data obtained were corrected for dilution. In fluorimetric titrations, an excitation wavelength of $\lambda_{max} = 440$ nm was used (where possible checked with $\lambda_{exc} = 320$ nm) and changes in emission at maxima (Table 1) were monitored. The binding constants and stoichiometries of complexes of **6–8** with the nucleotides were calculated from the concentration range corresponding to ca 20–80% complexation by the non-linear least-squares fitting program SPECFIT.[20] The binding constants (K_s) of **6–8** toward polynucleotides and [bound ligand]/[polynucleotide phosphate] ratio (n) were calculated according to the Scatchard equation[18] by a non-linear least-squares fitting method. Values for K_s and n given in the text (*ct* DNA) and in Table 4 all have satisfactory correlation coefficients (>0.999).

*8-(Propyl)amino-5,6-dimethylphenanthridinium triflate (**1**).* 8-(Propyltosyl)amino-6-methylphenanthridine[10] (230 mg, 0.57 mmol) and $CF_3SO_3CH_3$ (190 µl, 1.71 mmol) were dissolved in dry 1,2-dichloroethane (5 ml) and stirred for 4 days under an argon atmosphere at room temperature. CF_3SO_3H (180 µl, 1.9 mmol) was added and the reaction mixture was stirred for 2 days. After solvent removal, a brown oil was obtained and purified by TLC (SiO_2, 10% MeOH in CH_2Cl_2, $R_f = 0.65$) to give a red powder of **1** (110 mg, 46%) that was recrystallized from CH_3CN.

*8-[3-(Urac-1-yl)propyl]amino-5,6-dimethylphenanthridinium triflate (**2**).* 8-(3-(Urac-1-yl)propyltosyl)(amino-6-methylphenanthridine[10] (280 mg, 0.54 mmol) and $CF_3SO_3CH_3$ (180 µl, 1.63 mmol) were dissolved in dry 1,2-dichloroethane (7 ml) and stirred for 2 days under an argon atmosphere at room temperature. CF_3SO_3H (70 µl, 0.81 mmol) was added and the reaction mixture stirred for 2 h. After solvent removal, a brown oil was obtained and purified by TLC (SiO_2, 20% MeOH in CH_2Cl_2, $R_f = 0.16$) to give a red powder of **2** (21 mg, 8%) that was recrystallized from CH_3CN.

*8-(3-Bromopropyltosyl)amino-5,6-dimethylphenanthridinium triflate (**3**).* 8-(3-Bromopropyltosyl)amino-6-methylphenanthridine[10] (500 mg, 1.05 mmol) and $CF_3SO_3CH_3$ (230 µl, 2.07 mmol) were dissolved in dry 1,2-dichloroethane (10 ml) and stirred for 1 day under an argon atmosphere at room temperature. After solvent removal, a brown oil was obtained and purified by TLC (SiO_2, 10% MeOH in CH_2Cl_2, $R_f = 0.47$) to give a light yellow oil of **3** (350 mg, 52%).

*8-[3-(Aden-9-yl)propyltosyl] amino-5,6-dimethylphenanthridinium triflate (**4**).* Adenine (157 mg, 1.16 mmol) that was previously dried and NaH (46 mg, 60% w/w, 1.16 mmol), were suspended in dry DMF (10 ml) and stirred for 1 h under an argon atmosphere at room temperature. To this suspension, a solution of triflate **3** (250 mg, 0.386 mmol) in dry DMF (20 ml) was added dropwise and the reaction mixture was stirred in the dark for 24 h under an argon atmosphere at room temperature. After solvent removal, the residue was suspended in CH_2Cl_2, filtered and washed several times with CH_2Cl_2. The solution was concentrated and purified by TLC (SiO_2, 20% MeOH in CH_2Cl_2, $R_f = 0.1$) to give a light gray solid of **4** (50 mg, 18%).

*8-[3-(Aden-9-yl)propyl]amino-5,6-dimethylphenanthridinium triflate (**5**).* Triflate **4** (50 mg, 0.07 mmol) was suspended in dry 1,2-dichloroethane (5 ml), then CF_3SO_3H (12 µl, 0,14 mmol) was added and stirred for 1 h under an argon atmosphere at room temperature. After solvent removal, the oily residue was crystallized from MeOH–CH_3CN–diethyl ether to give an orange powder of **5** (32 mg, 80%).

*8-(Propyl)amino-5,6-dimethylphenanthridinium hydrogensulfate (**6**).* To a solution of triflate **1** (100 mg, 0.24 mmol) in dry CH_3CN (1 ml), a solution of tetrabutylammonium hydrogensulfate (1.6 g, 4.8 mmol) in dry CH_3CN (1 ml) was added. The precipitated product was collected by filtration to give a red powder of **6** (60 mg, 69%).

*8-[3-(Urac-1-yl)propyl]amino-5,6-dimethylphenanthridinium hydrogensulfate (**7**).* Compound **7** was obtained as described for **6**; triflate **2** (15 mg, 0.03 mmol) and tetrabutylammonium hydrogensulfate (260 mg, 0.76 mmol) in dry CH_3CN (1 + 1 ml) gave an orange powder of **7** (4 mg, 30%).

*8-[-(Aden-9-yl) propyl]amino-5,6-dimethylphenanthridinium hydrogensulfate (**8**).* Compound **8** was obtained as described for **6**; triflate **5** (7 mg, 0.01 mmol) and tetrabutylammonium hydrogensulfate (8 mg, 0.02 mmol) in dry CH_3CN (1 + 1 ml) gave an orange powder of **8** (4 mg, 57%).

Molecular modeling. The model of the four ds-polyA^+ pairs was built and optimized using two-layer ONIOM[21] calculations with the Gaussian 98[22] program. Methods in the ONIOM calculations were UFF[23] for a lower layer and the density functional method (DFT) B3LYP/3–21G*[24] for a higher layer. Subsequently a second model was built from the optimized ds-polyA^+ units and **8**, which was manually docked between ds-polyA^+ units. Subsequent geometry optimizations for the second model were also carried out.

To achieve the required computational accuracy and to satisfy the computer time demands, the higher layer, optimized at the DFT level, consisted of four protonated adenine rings in the middle of the constructed model and the entire compound **8**, while the remaining parts of the model were in the lower layer and calculated by the UFF method. No constraints or restraints were applied to the model.

REFERENCES

1. Chastain M, Tinoco I Jr. In *Progress in Nucleic Acid Research and Molecular Biology*, vol. 41, Cohn WE, Moldave K (eds). Academic Press: New York, 1991; 131–177.
2. (a) Saenger W. *Principles of Nucleic Acid Structure*. Springer: New York, 1988; (b) Cantor CR, Schimmel PR. In *Biophysical Chemistry*, vol. 3. Freeman: San Francisco, 1980; 1109–1181.
3. (a) Lhomme J, Constant J-F, Demeunynck M. *Biopolymers* 1999; **52**: 65–83; (b) Chaudhry MA, Weinfeld M. *J. Biol. Chem.* 1997; **272**: 15650–15655; (c) Naegeli H. *Mechanism of DNA Damage Recognition in Mammalian Cells*. R. G. Landes: Austin, TX and Springer: Heidelberg, 1997; (d) Wood RD. *Annu. Rev. Biochem.* 1996; **65**: 135–167.
4. Hemminki K, Ludlum DB. *J. Natl. Cancer Inst.* 1984; **73**: 1021–1028.
5. (a) Demeunynck M, Bailly C, Wilson WD. *DNA and RNA Binders*. Wiley-VCH: Weinheim, 2002; (b) Barret JM, Etievant C, Fahy J, Lhomme J, Hill BT. *Anticancer Drugs* 1999; **10**: 55–65.
6. Cuniasse P, Fazakerley GV, Guschlbauer W, Kaplan BE, Sowers LC. *J. Mol. Biol.* 1990; **213**: 303–314.
7. (a) Nissen JP, Hansen N, Ban PB, Moore, Steitz TA. *Science* 2000; **289**: 920–930; (b) Muth GW, Ortoleva-Donnelly L, Strobel SA. *Science* 2000; **289**: 947–950; (c) Ravindranathan S, Butcher SE, Feigon J. *Biochemistry* 2000; **51**: 16026–16032; (d) Kettani A, Gueron M, Leroy J-L. *J. Am. Chem. Soc.* 1997; **119**: 1108–1115; (e) Sugimoto N, Wu P, Hara H, Kawamoto Y. *Biochemistry* 2001; **31**: 9396–9405; (f) Asensio JL, Lane AN, Dhesi J, Bergqvist S, Brown T. *J. Mol. Biol.* 1998; **275**: 811–822.
8. (a) Fkyerat A, Demeunynck M, Constant J-F, Michon P, Lhomme J. *J. Am. Chem. Soc.* 1993; **115**: 9952–9959; (b) Fkyerat A, Demeunynck M, Constant J-F, Lhomme J. *Tetrahedron* 1993; **49**: 11237–11252; (c) Berthet N, Boudali A, Constant J-F, Decout J-L, Demeunynck M, Fkyerat A, Garcia J, Laayoun A, Michon P, Lhomme J. *J. Mol. Recog.* 1994; **7**: 99–107; (d) Belmont P, Boudali A, Constant J-F, Demeunynck M, Fkyerat A, Michon P, Serratrice G, Lhomme J. *New J. Chem.* 1997; **21**: 47–54; (e) Coppel Y, Constant J-F, Coulombeau C, Demeunynck M, Garcia J, Lhomme J. *Biochemistry* 1997; **36**: 4831–4843; (f) Belmont P, Jourdan M, Demeunynck M, Constant J-F, Garcia J, Lhomme J, Carez D, Croisy A. *J. Med. Chem.* 1999; **42**: 5153–5159; (g) Alarcon K, Demeunynck M, Lhomme J, Carrez D, Croisy A. *Bioorg. Med. Chem.* 2001; **9**: 1901–1910.
9. Constant J-F, Fahy J, Lhomme J. *Tetrahedron Lett.* 1987; **28**: 1777–1780.
10. Tumir L-M, Piantanida I, Novak P, Žinić M. *J. Phys. Org. Chem.* 2002; **15**: 599–607.
11. Juranović I, Meić Z, Piantanida I, Tumir L-M, Žinić M. *J. Chem. Soc., Chem. Commun.* 2002; 1432–1433.
12. Yajima H, Fujii N, Ogawa H, Katawani H. *J. Chem. Soc., Chem. Commun.* 1974; 107–108.
13. Čudić P, Žinić M, Tomišić V, Simeon V, Vigneron J-P, Lehn J-M. *J. Chem. Soc., Chem. Commun.* 1995; 1073–1075.
14. Davies DB, Veselkov AN. *J. Chem. Soc., Faraday Trans.* 1996; **92**: 3545–3557.
15. Odani A, Masuda H, Yamauchi O, Ishiguro S. *Inorg. Chem.* 1991; **30**: 4486–4488.
16. Piantanida I, Tomišić V, Žinić M. *J. Chem. Soc., Perkin Trans. 2* 2000; 375–383.
17. Piantanida I, Palm BS, Žinić M, Schneider H-J. *J. Chem. Soc., Perkin Trans. 2* 2001; 1808–1816.
18. (a) Scatchard G. *Ann. N.Y. Acad. Sci. 1949;* **51**: 660–664; (b) McGhee JD, von Hippel PH. *J. Mol. Biol.* 1974; **86**: 469–489.
19. Zimmermann HW. *Angew. Chem., Int. Ed. Engl.* 1986; **25**: 115–196.
20. *Specfit Global Analysis, a Program for Fitting Equilibrium and Kinetic Systems, using Factor Analysis & Marquardt Minimization*; Gampp H, Maeder M, Meyer CJ, Zuberbuehler AD. *Talanta* 1985; **32**: 257; Maeder M, Zuberbuehler AD. *Anal. Chem.* 1990; **62**: 2220–2224.
21. Maseras F, Morokuma K. *J. Comput. Chem.* 1996; **16**: 1170–1179.
22. Frisch MJ, Trucks GW, Schlegel HB, Scuseria GE, Robb MA, Cheeseman JR, Zakrzewski VG, Montgomery JA Jr, Stratmann RE, Burant JC, Dapprich S, Millam JM, Daniels AD, Kudin KN, Strain MC, Farkas O, Tomasi J, Barone V, Cossi M, Cammi R, Mennucci B, Pomelli C, Adamo C, Clifford S, Ochterski J, Petersson GA, Ayala PY, Cui Q, Morokuma K, Salvador P, Dannenberg JJ, Malick DK, Rabuck AD, Raghavachari K, Foresman JB, Cioslowski J, Ortiz JV, Baboul AG, Stefanov BB, Liu G, Liashenko A, Piskorz P, Komaromi I, Gomperts R, Martin RL, Fox DJ, Keith T, Al-Laham MA, Peng CY, Nanayakkara A, Challacombe M, Gill PMW, Johnson B, Chen W, Wong MW, Andres JL, Gonzalez C, Head-Gordon M, Replogle ES, Pople JA. *Gaussian 98, Revision A.11*. Gaussian, Inc., Pittsburgh PA, 2001.
23. Rappe AK, Casewit CJ, Colwell KS, Goddard WA III, Skiff WM. *J. Am. Chem. Soc.* 1992; **114**: 10024–10035.
24. Becke AD. *J. Chem. Phys.* 1993; **98**: 5648–5652.